Similarity solutions for spreading of a two-dimensional non-Newtonian gravity current in a porous layer

Vittorio Di Federico [a,*], Renata Archetti [a], Sandro Longo [b]

[a] Dipartimento di Ingegneria Civile, Ambientale e dei Materiali (DICAM), Università di Bologna, Italy
[b] Dipartimento di Ingegneria Civile, Ambiente Territorio e Architettura (DICATeA), Università di Parma, Italy

ABSTRACT

We consider the motion of shallow two-dimensional gravity currents of a purely viscous and relatively heavy power-law fluid of flow behavior index n in a uniform saturated porous layer above a horizontal impermeable boundary, driven by the release from a point source of a volume of fluid increasing with time like t^{α}. The equation of motion for power-law fluids in porous media is a modified Darcy's law taking into account the nonlinearity of the rheological equation. Coupling the flow law with the mass balance equation yields a nonlinear differential problem which admits a self-similar solution describing the shape of the current, which spreads like $t^{(\alpha+n)/(2+n)}$, generalizing earlier results for Newtonian fluids. For the particular values $\alpha = 0$ and 2, closed-form solutions are derived; else, a numerical integration is required; the numerical scheme is tested against the analytical solutions. Two additional analytical approximations, valid for any α, are presented. The space-time development of the gravity current is discussed for different flow behavior indexes.

© 2012 Elsevier B.V. All rights reserved.

1. Introduction

Gravity-driven flows in porous media occur when a fluid of one density intrudes into a man-made or natural porous formation saturated with fluid of a different density. The flow, which is predominantly horizontal, is driven by gravity acting on the different densities. Important examples include fluid injection in geothermal reservoirs [1], displacement flows in oil reservoirs [2], injection of brines for groundwater cleanup [3], and carbon sequestration [4,5]. When the interface between the two fluids remains well-defined, a description of its displacement is of great practical interest, as shown by the ample literature on single-phase gravity currents in porous media. For their study, a number of analytical and/or numerical solutions were developed under a variety of conditions: flow over an horizontal impermeable surface in plane [6] or radial geometry [7], motion over a sloping bottom [8], flow in fractured media [9], flow over an inclined plane within confining boundaries [10]; the solutions were often validated against experimental observation. Many analytical approaches focused on deriving similarity solutions governing the short- or long-term spreading of the current, in analogy with the general literature on gravity currents in the environment [11–15].

Several fluids used in the process and oil industries, as well as in environmental and remediation applications, display non-Newtonian behavior [16–18].

In petroleum engineering, heavy and waxy oils are often found to exhibit non-Newtonian characteristics at reservoir conditions [19]. Fluids used to enhance oil recovery from underground reservoirs frequently exhibit shear-dependence of viscosity and other distinctly non-linear effects, due to the addition of chemical additives, polymeric solutions or foams to the injected water to improve the overall sweeping efficiency and minimize the instability effects [16,20,21].

Environmental contaminants of emerging concern such as greases, sludges, slurries, asphalts, bitumens, drilling fluids and oil, often deviate from Newtonian behavior [22]. Nonlinear rheological properties are also displayed by colloidal substances [23] or biosuspensions [24] injected into contaminated soils to remove liquid pollutants.

It is therefore of interest to extend the study of gravity currents in porous media to the non-Newtonian case, in order to investigate the impact of the nonlinearity of the flow law on the current spreading. We do so for a power-law fluid, whose motion is described by a modified Darcy's law taking into account the nonlinearity of the rheological equation, and for a plane current driven by the instantaneous or maintained injection of a volume of fluid. A solution to the problem is derived in self-similar form, generalizing the approach adopted for Newtonian fluids [6,7]. An analogous solution was obtained in [25] for injection in a porous medium at

* Corresponding author.
E-mail addresses: vittorio.difederico@unibo.it (V. Di Federico), renata.archetti@unibo.it (R. Archetti), sandro.longo@unipr.it (S. Longo).

assigned fluid depth and in [26] for release of a constant volume in radial geometry.

As implied earlier, in our analysis of the displacement phenomenon we assume the absence of fingering instabilities, described in the classical paper by Saffman and Taylor [27]. In the review by Homsy [28] three patterns of instabilities are analysed in deeper detail: (1) instabilities driven by the difference in viscosity and influenced by the diffusive mixing between the fluids; (2) instabilities driven by both gravity and viscosity; (3) instabilities resulting when a low-viscosity Newtonian fluid is injected from a source in a porous medium filled with a miscible but strongly non-Newtonian fluid. This last pattern, albeit not relevant to the present study, incorporates a non-Newtonian nature at least of one of the two fluids. More recently, the peculiar nature of Saffman–Taylor instability for non-Newtonian fluids was studied experimentally for polymer solutions described by the power-law model [29], and theoretically for different constitutive equations in [30]. In general, viscous fingering involving non-Newtonian fluids is receiving a lot of attention in the literature, but much effort is still needed, also because the variety of possible combinations of different rheological models is extremely wide.

The present paper is organized as follows. In section 2, the formulation of the flow law for a non-Newtonian power-law fluid is reviewed. In section 3 the problem is formulated and solved in dimensionless form via analytical/numerical methods; results for shape factors, current length and profile are discussed as functions of flow behavior index and type of injection. Two methods to derive an approximate analytical solution to the general problem and a particular solution valid for inflow rate linearly increasing with time are then presented. A further discussion and conclusions are reported in section 4.

2. Flow law for non-Newtonian fluid flow in a porous medium

The non-Newtonian fluid is described by the rheological Ostwald–deWaele power-law model, given for simple shear flow by

$$\tau = m\dot{\gamma}|\dot{\gamma}|^{n-1}, \tag{1}$$

in which τ is the shear stress, $\dot{\gamma}$ the shear rate, m the fluid consistency index (dimensions $[ML^{-1}T^{n-2}]$) and n the flow behavior index (a positive real number). When $n < 1$, $=1$ or >1 the model describes respectively shear-thinning, Newtonian, or shear-thickening behavior. The power-law model is a simplification of more complex stress-shear rate relationship: for fluids flowing in porous media this includes effects such as time-dependent behavior [18], a Newtonian plateau in the apparent viscosity for low shear rates [16], nonzero yield stress [19]. Nevertheless, in many instances the model represents well the behavior of fluids of interest over a considerable range of shear rates, and is a good approximation of a Herschel–Bulkley model for vanishing values of the yield stress.

The flow law for the fluid is a modified Darcy's law taking into account the nonlinearity of the rheological Eq. (1), originally proposed in [31], retaken and verified experimentally by [32], and later adopted by other authors [16,25,33–39]

$$\nabla P = -\frac{\mu_{eff}}{k}|\mathbf{u}|^{n-1}\mathbf{u}, \tag{2}$$

where $P = p + \rho g z$ is the generalized pressure, p the pressure, z the vertical coordinate, ρ the fluid density, g the specific gravity, $\mathbf{u}$ the Darcy velocity $[LT^{-1}]$, k the intrinsic permeability coefficient $[L^2]$, and μ_{eff} the effective viscosity $[ML^{-n}T^{n-2}]$; the mobility ratio k/μ_{eff} is a function of m, k, ϕ, n according to [35]

$$\frac{k}{\mu_{eff}} = \frac{1}{2m}\left(\frac{n\phi}{3+n}\right)^n\left(\frac{8k}{\phi}\right)^{(1+n)/2}, \tag{3}$$

where ϕ denotes the porosity. For $n = 1$, the effective viscosity μ_{eff} reduces to conventional viscosity μ $[ML^{-1}T^{-1}]$, and Eq. (2) reduces to Darcy's law $\nabla P = -(\mu/k)\mathbf{u}$. Alternative formulations of the flow law retaining the same structure of (2) have been proposed in the literature: according to [40–45] $\nabla P = -(m/k^*)|\mathbf{u}|^{n-1}\mathbf{u}$, where k^* is the generalized permeability having dimensions $[L^{n+1}]$; upon comparing the latter expression with (2) it is seen that $\mu_{eff}/k = m/k^*$. A macroscopic law of the form (2) was obtained for power-law fluid flow by [46] via numerical simulations of at the pore scale based on smoothed particle hydrodynamics, and by [47] with network modeling. In [48], the nonlinear flow law is written as $\mathbf{u} = -K|\mathbf{u}|^{1-n}\nabla P$, where K $[M^{-1}L^{(2+n)}T^{(2-n)}]$ is a function of n.

It is convenient to write (2),(3) as [49]

$$\nabla P = -\frac{1}{\Lambda k^{(1+n)/2}}|\mathbf{u}|^{n-1}\mathbf{u},$$
$$\Lambda = \Lambda(\phi, m, n) = \frac{8^{(n+1)/2}}{2}\left(\frac{n}{3n+1}\right)^n\frac{\phi^{(n-1)/2}}{m} \tag{4}$$

highlighting the dependence upon permeability k.

3. Problem formulation

Consider the motion of a two-dimensional (plane) gravity current of a non-Newtonian fluid of uniform density ρ introduced at the base of a porous medium layer of depth h_0, saturated with immiscible fluid of uniform density $\rho - \Delta\rho$, above a horizontal impermeable boundary as sketched in Fig. 1.

The gravity current has a height $h(x,t)$ and extends to a coordinate denoted by $x_N(t)$; any secondary motion induced by the current is considered to be negligible, on the assumption that the overall domain thickness is decidedly larger than that of the intruding layer, and the corresponding velocity much smaller.

Indicating with u and w the Darcy velocities in the x and z direction, a balance of terms in the continuity equation $\partial u/\partial x + \partial w/\partial z = 0$ yields $w \approx \varepsilon u$, where ε is the current depth/length ratio; assuming $\varepsilon \ll 1$ (a thin intruding current) leads to first-order to motion parallel to the boundary. Then the Darcy velocity in the x direction is given by the one-dimensional counterpart of Eq. (4), which reads for horizontal flow with $\partial p/\partial x < 0$

$$u(x,t) = \left(-\Lambda k^{(1+n)/2}\frac{\partial p}{\partial x}\right)^{1/n}. \tag{5}$$

In the shallow water approximation, the pressure within the intruding fluid layer ($0 \leqslant z \leqslant h$) is hydrostatic and given by [6,7]
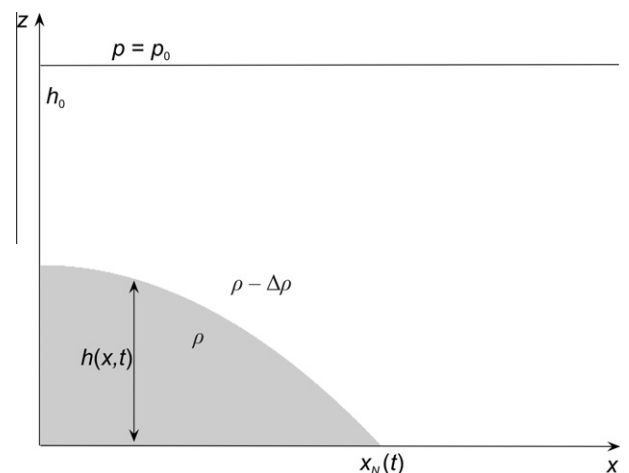

Fig. 1. Sketch of the gravity current of density ρ and height $h(x,t)$ intruding into a porous medium saturated with fluid of density $\rho - \Delta\rho$.

$$p(x,z,t) = p_1 + \Delta\rho g h(x,t) - \rho g z, \qquad (6)$$

where $p_1 = p_0 + (\rho - \Delta\rho)gh_0$ is a constant, and p_0 is the constant pressure at $z = h_0$. The pressure gradient driving the flow is thus related to the gradient of the unknown free surface by

$$\frac{\partial p}{\partial x} = \Delta\rho g \frac{\partial h}{\partial x}, \qquad (7)$$

where any capillary forces (surface tension) between the two fluids have been neglected; hence there is no capillary entry pressure limiting the migration of the injected fluid through the pores of the medium. Introducing Eq. (7) into Eq. (5), we find that

$$u(x,t) = (\Lambda\Delta\rho g)^{1/n} k^{(1+n)/2n} \left(-\frac{\partial h}{\partial x} \right)^{1/n}. \qquad (8)$$

For one dimensional transient flow, the local continuity condition takes the form [6]

$$\frac{\partial}{\partial x}(uh) = -\phi \frac{\partial h}{\partial t}. \qquad (9)$$

Substituting Eq. (8) into Eq. (9), we obtain the nonlinear partial differential equation governing the unknown free-surface height $h(x,t)$

$$\frac{(\Lambda\Delta\rho g)^{1/n} k^{(1+n)/2n}}{\phi} \frac{\partial}{\partial x}\left[h\left(-\frac{\partial h}{\partial x} \right)^{1/n} \right] = -\frac{\partial h}{\partial t}. \qquad (10)$$

Consider the flux to be such that the total volume per unit width of the dense fluid in the porous medium at any time is given by $q_p t^\alpha$, where both $q_p[L^2 T^{-\alpha}]$ and α are constant; a value $\alpha = 0$ implies an instantaneous release of a fixed volume per unit width q_p, while $\alpha = 1$ indicates the release at a constant volume flux. The global mass balance equation then reads

$$\phi \int_0^{x_N(t)} h(x,t)dx = q_p t^\alpha. \qquad (11)$$

The mathematical statement of the problem is completed by the boundary condition

$$h(x_N(t),t) = 0. \qquad (12)$$

Eqs. (10)–(12) may be non-dimensionalized by setting

$$T = \frac{t}{t^*}, \quad X = \frac{x}{x^*}, \quad X_N = \frac{x_N}{x^*}, \quad H = \frac{h}{x^*}, \qquad (13)$$

where the time, space, and velocity scales are

$$t^* = \left(\frac{q_p}{\phi V^2} \right)^{1/(2-\alpha)}, \quad x^* = V \cdot t^*, \quad V = (\Lambda\Delta\rho g)^{1/n} k^{(1+n)/2n}/\phi, \qquad (14)$$

thereby generalizing to non-Newtonian case the choice of [8]; the special case $\alpha = 2$ will be covered later in Section 3.2.

This recasts Eqs. (10) and (11), respectively, in the following dimensionless form

$$\frac{\partial}{\partial X}\left[H\left(-\frac{\partial H}{\partial X} \right)^{1/n} \right] = -\frac{\partial H}{\partial T}, \qquad (15)$$

$$\int_0^{X_N} H dX = T^\alpha, \qquad (16)$$

while Eq. (12) is unchanged in dimensionless variables. We then introduce the similarity variable

$$\zeta = XT^{-(\alpha+n)/(2+n)}, \qquad (17)$$

and denote the value of ζ for $X = X_N(T)$ by ζ_N. Then the similarity solution of Eqs. (15),(16) with Eq. (12) is of the form

$$H(X,T) = \zeta_N^{(n+1)} T^{[\alpha(n+1)-n]/(2+n)} \Phi(\zeta), \quad \zeta = \xi/\xi_N, \qquad (18)$$

with ζ being the reduced similarity variable. Substituting Eqs. (17) and (18) in Eq. (15) yields

$$\frac{d}{d\zeta}\left[\Phi\left(-\frac{d\Phi}{d\zeta} \right)^{1/n} \right] - \frac{\alpha+n}{2+n}\zeta\frac{d\Phi}{d\zeta} + \frac{\alpha(n+1)-n}{2+n}\Phi = 0, \qquad (19)$$

while Eqs. (16) and (12) transform respectively into

$$\xi_N = \left(\int_0^1 \Phi(\zeta)d\zeta \right)^{-1/(2+n)}, \qquad (20)$$

$$\Phi(\zeta = 1) = 0. \qquad (21)$$

Once ξ_N is determined, the (dimensionless) length of the gravity current at a given time is given by

$$X_N(T) = \xi_N T^{(\alpha+n)/(2+n)}. \qquad (22)$$

For $n = 1$, governing equations and results reduce to those derived for a Newtonian fluid by Huppert and Woods [6] in dimensional form. It follows from (22) that the velocity of the current tip is proportional to $T^{(\alpha-2)/(2+n)}$, i.e. the current accelerates or decelerates depending whether $\alpha > 2$ or $\alpha < 2$.

In the case $\alpha = 0$ (instantaneous release of a fixed amount of fluid), the problem is amenable to an analytical solution. Assuming a solution of the form $\Phi(\zeta) = a(1 - \zeta^b)$, which satisfies the boundary condition (21), substituting in Eq. (19) and equating the exponents in order to have equal order monomials, the exponent b is first evaluated; then equating the coefficients of the equal order monomials the coefficient a is computed and the following analytical solution is obtained:

$$\Phi(\zeta) = \frac{n^n}{(2+n)^n(1+n)}(1 - \zeta^{n+1}) \quad \text{and} \quad \xi_N = \left[\frac{n^n}{(2+n)^{n+1}} \right]^{-1/(2+n)}. \qquad (23)$$

For a Newtonian fluid, Eq. (23) reduce to Eq. (3.7) in [6]. Integrating Eq. (19) between ζ and one results in

$$\left(-\frac{d\Phi}{d\zeta} \right)^{1/n} - \frac{\alpha+n}{2+n}\zeta - \frac{\alpha}{\Phi}\int_\zeta^1 \Phi d\zeta = 0. \qquad (24)$$

In the limit $\alpha \to 0$ the last term is null and Eq. (24) can be directly integrated yielding the solution (23).

In the limit $\zeta \to 1$ the last term is still null because the integral is a polynomial of higher order than the denominator, hence one obtains

$$\left. \frac{d\Phi}{d\zeta} \right|_{\zeta\to1} = -\left(\frac{\alpha+n}{2+n} \right)^n, \qquad (25)$$

while the limit $\zeta \to 0$ leads to

$$\left. \frac{d\Phi}{d\zeta} \right|_{\zeta\to0} = -\frac{\alpha^n}{\Phi^n}\left(\int_0^1 \Phi d\zeta \right)^n. \qquad (26)$$

In the case of arbitrary α (except $\alpha = 2$, see Section 3.2), Eq. (19) can be solved numerically with the second boundary condition given by Eq. (25). Note that the condition expressed by Eq. (21) reduces the order of the differential equation introducing an irregular behavior of the solution near the current tip. To handle this singularity we consider the first order solution near the current tip obtained integrating Eq. (25):

$$\Phi(\zeta \to 1 - \varepsilon) = \left(\frac{\alpha+n}{2+n} \right)^n \varepsilon + O(\varepsilon^2), \qquad (27)$$

where ε is a small quantity. By assuming

$$\Phi(\zeta \to 1 - \varepsilon) = \left(\frac{\alpha + n}{2 + n}\right)^n \varepsilon,$$

$$\left.\frac{d\Phi}{d\zeta}\right|_{\zeta \to 1 - \varepsilon} = -\left(\frac{\alpha + n}{2 + n}\right)^n, \tag{28}$$

with $\varepsilon \to 0$, the singular regular point is handled. The numerical integration of Eq. (19) with boundary conditions (28) in the domain $[0, 1 - \varepsilon]$ is performed by using Wolfram Mathematica® 7 routines, with 20 digits of accuracy and 20 digits of precision in the final result and 25 digits of precision in internal computations; the correctness of the numerical results is checked by comparison with the analytical solution, obtaining an error of order ε^2 as expected.

The resulting shape factors Φ are illustrated in Fig. 2 for different values of flow behavior index n and parameter α, together with the analytical solution for $\alpha = 0$.

The shape factors in Fig. 2 increase with α, due to the larger volume released into the domain, and moderately decrease with increasing n. In the origin the shape factor is horizontal only for $\alpha = 0$, as shown by Eq. (26); this is because the mass flux continually introduced for $\alpha > 0$ induces a surface slope in the origin. When compared to results valid for free surface flows (see [11] for the Newtonian case, and [50] for the non-Newtonian one), the shape factors in Fig. 2 exhibit a difference in their slope at the current tip ($\zeta = 1$); in a porous medium said slope has a finite value, decreasing with increasing n, while free-surface shape factors have a vertical tangent in $\zeta = 1$.

The similarity variable at the current tip ξ_N, evaluated from the numerical solution using Eq. (20), is depicted in Fig. 3 as a function of α. ξ_N shows lower values for shear-thinning than for shear-thickening fluids when $\alpha < 1$; the reverse is true for $\alpha > 1$; the dependence of ξ_N on the value of flow behavior index n is modest.

The time evolution of the current length X_N is shown in Fig. 4 for an instant release of fluid ($\alpha = 0$) and for constant fluid inflow rate ($\alpha = 1$), i.e. the two most realistic release conditions, considering different values of n. In both cases, for $T < 1$, the current head advances farther as n decreases; the reverse is true for $T > 1$.

Figs. 5 and 6 show the profiles of the current at different times and values of n, respectively for $\alpha = 0$ and 1. For the case of an instantaneous injection shown in Fig. 5, the released fluid volume slumps down more rapidly for shear-thickening gravity currents
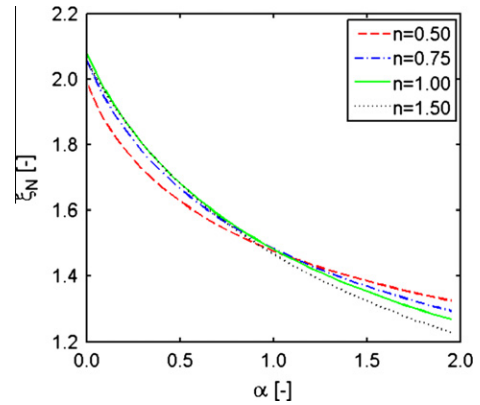

Fig. 3. Values of ξ_N as a function of α for different values of the flow behavior index n.

than for Newtonian or shear-thinning ones. As a result, depth profiles of the former are more elongated than profiles of the latter; the same behavior was observed for free surface gravity currents of power-law fluids [50]. When a constant inflow rate is considered (Fig. 6), the former observation still holds; the surface slope in the origin decreases for increasing flow behavior index.

3.1. Approximate solution for generic values α and n

In this section, we consider two different methods to obtain an approximate solution valid for generic values of α and n.

We first consider a series expansion of the shape factor near the current tip ($\zeta = 1$). Introducing the variable $\chi = 1 - \zeta$, Eq. (19) transforms into

$$-\frac{d}{d\chi}\left[\Phi\left(\frac{d\Phi}{d\chi}\right)^{1/n}\right] + \frac{\alpha + n}{2 + n}(1 - \chi)\frac{d\Phi}{d\chi} + \frac{\alpha(n+1) - n}{2 + n}\Phi = 0. \tag{29}$$

We look for the solution given by a Frobenius series,

$$\Phi(\chi) = \sum_{k=0}^{\infty} a_k \chi^{k+b} \text{ as } \chi \to 0, \tag{30}$$

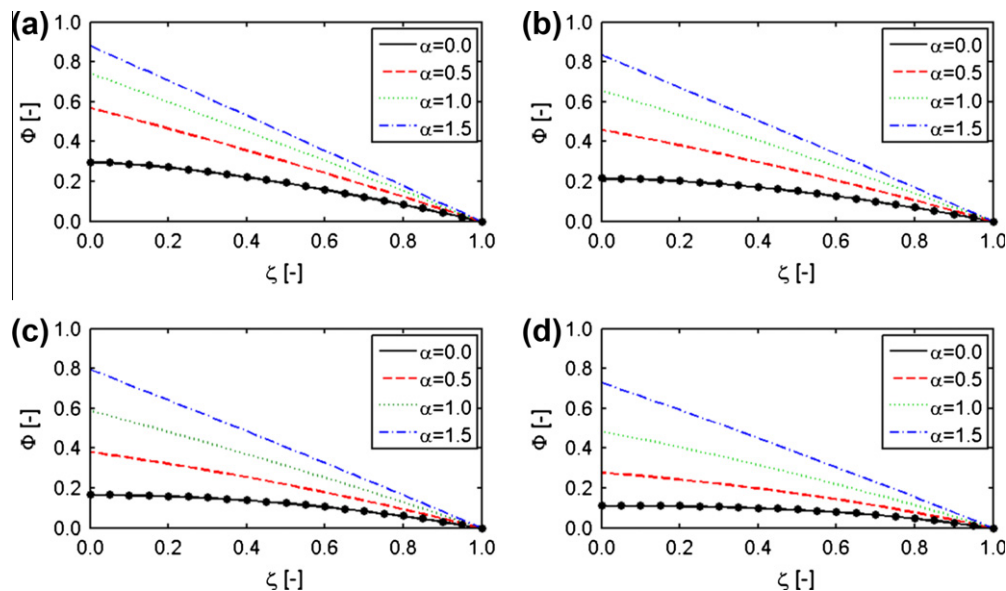Fig. 2. Shape factor Φ as a function of scaled similarity variable ζ for flow behavior index $n = 0.5$ (a), $n = 0.75$ (b), $n = 1.0$ (c) and $n = 1.5$ (d). Curves represent numerical solutions of (19) for α ranging between 0 and 1.5; dots represent the analytical solution (23).
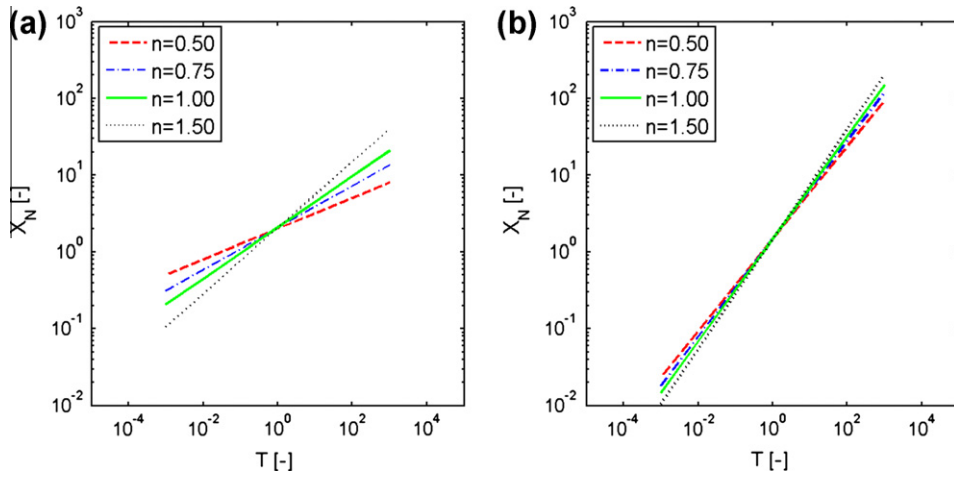
Fig. 4. Current length as a function of time for different values of flow behavior index n: (a) instantaneous release of fluid $\alpha = 0$; (b) constant inflow rate $\alpha = 1$.
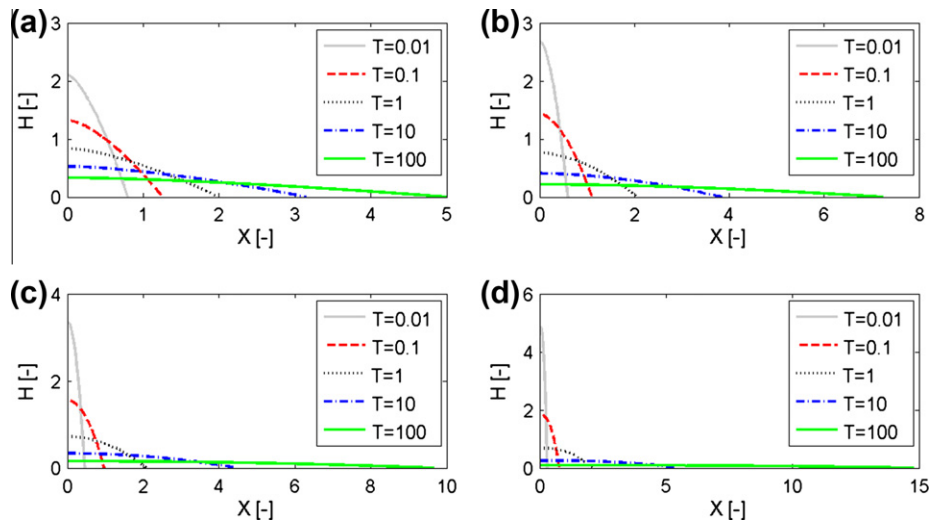

Fig. 5. Profiles of the current at different times for flow behavior index $n = 0.5$ (a), $n = 0.75$ (b), $n = 1.0$ (c) and $n = 1.5$ (d) for an instantaneous release of fluid ($\alpha = 0$).
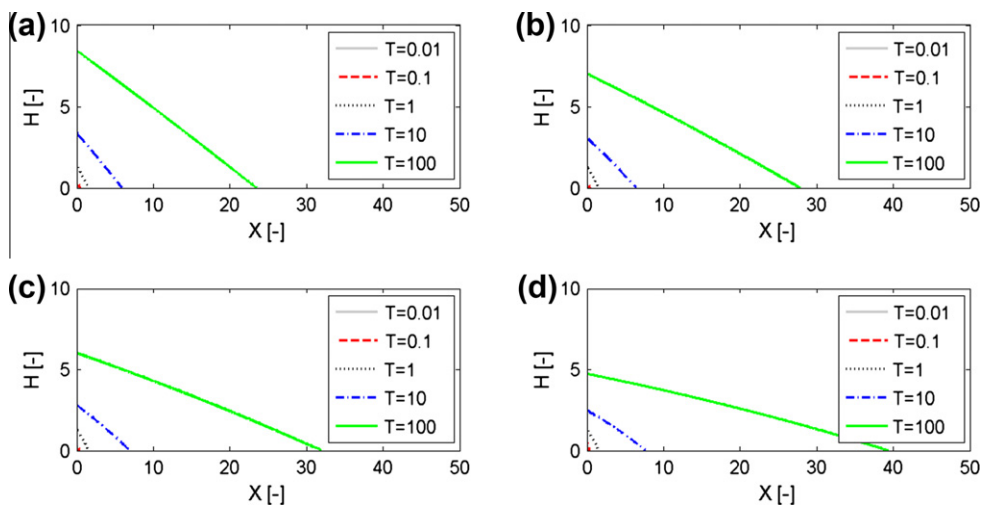

Fig. 6. Profiles of the current at different times for flow behavior index $n = 0.5$ (a), $n = 0.75$ (b), $n = 1.0$ (c) and $n = 1.5$ (d) for constant inflow rate ($\alpha = 1$).

where b is the indicial exponent. This series automatically satisfies the boundary condition $\Phi(\chi \to 0) = 0$. Its derivative and $1/n$ power are respectively equal to

$$\frac{d\Phi}{d\chi} = \sum_{k=0}^{\infty} a_k (k+b) \chi^{k+b-1} \tag{31}$$

$$\left(\frac{d\Phi}{d\chi}\right)^{1/n} = \sum_{m_0, m_1, \dots m_k} \binom{1/n}{m_0, m_1, \dots, m_k} (a_0 b \chi^{b-1})^{m_0}$$
$$\cdot [a_1(b+1)\chi^{b}]^{m_1} \cdots [a_k(k+b)\chi^{k+b-1}]^{m_k} = a_0^{\frac{1}{n}} b^{\frac{1}{n}} \chi^{\frac{b-1}{n}} + \dots \tag{32}$$

where the summation is taken over all sequences of indices m_0 through m_k such that the sum of all m is $1/n$ and the symbol

$$\binom{1/n}{m_0, m_1, \dots, m_k} = \frac{(1/n)!}{m_0! m_1! \cdots m_k!} \tag{33}$$

is the multinomial coefficients expression. Substituting (31) (32), (33) in Eq. (29) the following expression is obtained:

$$-a_0^{\frac{n+1}{n}} b^{\frac{1}{n}} \left(\frac{b-1}{n} + b\right) \chi^{\frac{b-1}{n}+b-1} + \dots + \frac{n+\alpha}{2+n} \sum_{k=0}^{\infty} a_k(b+k) \chi^{b+k-1}$$
$$-\frac{n+\alpha}{2+n} \sum_{k=0}^{\infty} a_k(b+k) \chi^{b+k} + \frac{\alpha(1+n)-2n}{2+n} \sum_{k=0}^{\infty} a_k \chi^{(b+k)} = 0, \tag{34}$$

where for simplicity only the first term in the expansion of $(d\Phi/d\chi)^{1/n}$ is written in explicit form. Equating the lowest powers of χ (for $k = 0$) we find the indicial exponent to be $b = 1$.

Equating the coefficients of the different powers of χ to zero, all the coefficients a_k are derived. The first three are:

$$a_0 = f^n$$
$$a_1 = \frac{a_0 n(g-f)}{2(2+n)a_0^{1/n} - 2fn} \tag{35}$$
$$a_2 = \frac{a_1 n^2(2f-g) + 6a_0^{1/n-1} a_1^2}{3n\left[nf - a_0^{1/n}(3+n)\right]}$$

where

$$f = \frac{\alpha+n}{2+n}, g = \frac{\alpha(n+1)-n}{2+n}. \tag{36}$$

Fig. 7a compares the shape factor obtained integrating numerically (19) and by means of the approximate analytical solution with $k = 2$, 3 and 4, for the case $n = 2$ and $\alpha = 1$; Fig. 7b shows the deviation of the approximate analytical solution from the numerical one; for $k = 4$, the two results are practically coincident. Note that the series expansion (30) gives an excellent approximation of the solution in the whole domain, even though the Frobenius series is developed near the tip of the current. An analogous comparison conducted for other values of α and n yields similar results (not shown).

At the current tip $\zeta = 1$, the first derivative of the shape function takes the value:

$$\frac{d\Phi}{d\zeta}\bigg|_{\zeta=1} = -f^n \equiv -\left(\frac{\alpha+n}{2+n}\right)^n \tag{37}$$

coincident with the expression obtained by different arguments in Eq. (25).

An alternative approximation involves an expansion of Eq. (24) for small α followed by an integration by iteration [51] assuming
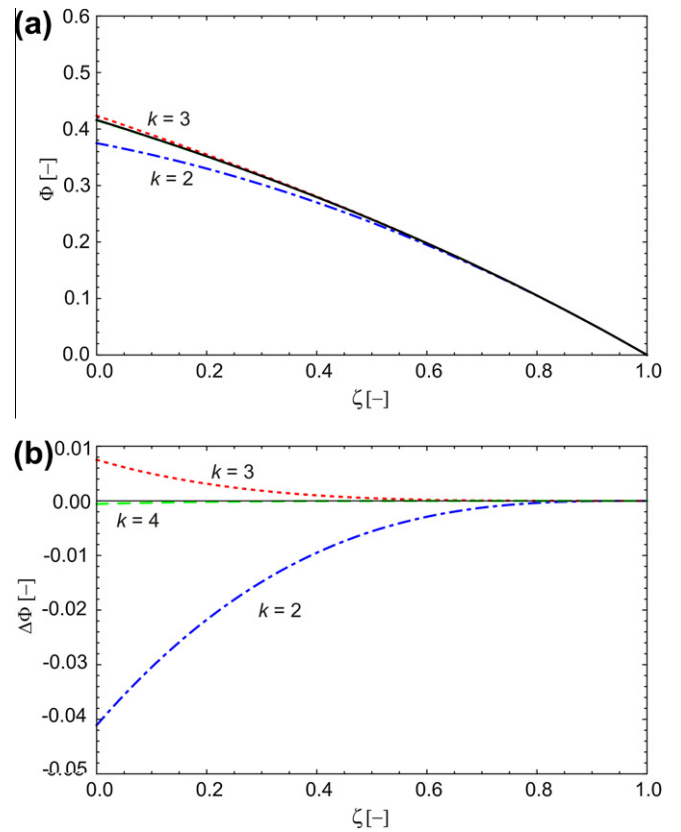

Fig. 7. (a) Shape factor Φ versus ζ obtained numerically and analytically with the Frobenius series approximation for $n = 2$, $\alpha = 1$. The bold line is the numerical integration, the dash-dot line, the dotted line and the dashed line are the series plots with 2, 3 and 4 terms. (b) Deviation between analytical and numerical results.

$$\frac{d\Phi_1}{d\zeta} = \left(-\frac{\alpha+n}{2+n}\zeta - \frac{\alpha}{\Phi_0} \int_{\zeta}^{1} \Phi_0 d\zeta\right)^n,$$
$$\frac{d\Phi_2}{d\zeta} = \left(-\frac{\alpha+n}{2+n}\zeta - \frac{\alpha}{\Phi_1} \int_{\zeta}^{1} \Phi_1 d\zeta\right)^n,$$
$$\dots$$
$$\frac{d\Phi_r}{d\zeta} = \left(-\frac{\alpha+n}{2+n}\zeta - \frac{\alpha}{\Phi_{r-1}} \int_{\zeta}^{1} \Phi_{r-1} d\zeta\right)^n, \tag{38}$$

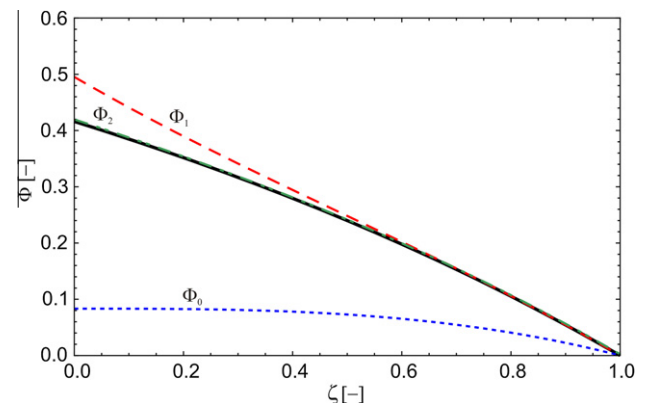**Fig. 8.** Shape factor Φ versus ζ obtained numerically and analytically with the integration by approximation for $n = 2$, $\alpha = 1$. The bold line is the numerical result, the dotted line is the analytical solution Φ_0 (23), the dashed line is the first iteration Φ_1. The second iteration Φ_2 is almost coincident with the numerical result.

where Φ_0 is the analytical solution for $\alpha = 0$, Φ_1 is the solution after the first iteration, and so on. The convergence is very fast, as shown in Fig. 8 for the case $n = 2$, $\alpha = 1$, where a single iteration gives a marked improvement over the analytical solution and a good agreement with the numerical one. The above approximation is of order α^{nr} with a better approximation for smaller values of α. The limitation of this method is the difficulty to solve analytically the integrals.

3.2. The special case $\alpha = 2$

We note that if $\alpha = 2$, the non-dimensional form given by Eq. (13) breaks down in the absence of the characteristic time scale defined in Eq. (14); further, an additional natural velocity scale arises beyond V defined in Eq. (14), namely $(q_p/\phi)^{1/2}$. We then define an arbitrary time scale $\tilde{t}^*$, a spatial length scale $\tilde{x}^* = (q_p/\phi)^{1/2}\tilde{t}^*$ and dimensionless variables $\tilde{T} = t/\tilde{t}^*$; $\tilde{X} = x/\tilde{x}^*, \tilde{X}_N = x_N/\tilde{x}^*, \tilde{H} = h/\tilde{x}^*$. In these new variables, the problem becomes

$$\delta_p \frac{\partial}{\partial \tilde{X}}\left[\tilde{H}\left(-\frac{\partial \tilde{H}}{\partial \tilde{X}}\right)^{1/n}\right] = -\frac{\partial \tilde{H}}{\partial \tilde{T}}$$

$$\int_0^{\tilde{X}_N} \tilde{H}d\tilde{X} = \tilde{T}^2,$$
(39)

where $\delta_p = V/(q_p/\phi)^{1/2}$ is the ratio between the two velocity scales in the problem. Defining the self-similar variable as $\xi = \tilde{X}/\tilde{T}$ and performing the same mathematical manipulations as in the general cases, the current height becomes $\tilde{H}(\tilde{X},\tilde{T}) = \xi_N^{n+1}T\Phi(\xi/\xi_N)$, where the shape factor Φ is given by

$$\delta_p \frac{d}{d\zeta}\left[\Phi\left(-\frac{d\Phi}{d\zeta}\right)^{1/n}\right] - \zeta\frac{d\Phi}{d\zeta} + \Phi = 0.$$
(40)

Eq. (40) with (20), (21) has the closed-form solution

$$\Phi = \left(\frac{1}{\delta_p}\right)^n (1-\zeta) \text{ and } \xi_N = (2\delta_p^2)^{1/(2+n)}.$$
(41)

The shape factors for this special case are shown in Fig. 9 for different values of flow behavior index n and parameter δ_p; its inspection shows that as δ_p increases, the shape factor decidedly decreases; this is so since δ_p represents the ratio between the product of factors favouring the current spreading (density difference, domain permeability, and reciprocal of porosity included in the definition of V)

and the source strength. The shape factor decreases with increasing n for $\delta_p \geqslant 1$; the reverse is true for $\delta_p < 1$.

4. Discussion and conclusions

We analyzed the horizontal spreading of non-Newtonian power-law gravity currents in a porous layer initially saturated with an ambient fluid of lower density for two-dimensional flow. The derived set of equations possesses self-similar, closed-form solutions for the instantaneous release of a fixed volume of fluid and for a linear increasing inflow rate ($\alpha = 2$). Setting the flow behavior index $n = 1$ reduces our solutions to those obtained earlier by [6].

The most interesting results are simple analytical solutions to a relatively complicated non-linear differential problems. These solutions can be used as a benchmark for the numerical algorithms and, by analogy, can be used for solving other similar physical problems. As for a Newtonian fluid [6] there are no undetermined parameters in the solution; this is a consequence of having neglected the motion of the external ambient fluid.

As for viscous free-surface gravity currents [11], the solution is completely independent on the details near the current tip, since the boundary conditions (28) are not externally imposed but derive from an analysis of the differential equation. Hence any further detailed analysis of the behavior near the current front shall affect the solution only locally, without modifying the current profile. We can infer that also for non-Newtonian flows in a porous medium this insensitivity to the front effects is limited to low Reynolds number and high Bond number (negligible effects of surface-tension).

The differential problem has a singularity in the origin, where the boundary condition induces a reduction of the order of the differential equation. The origin is a fixed regular singular point; hence following Fuchs Theorem (see [52]) at least one solution of the following form, which can be expressed as a Taylor series with a finite radius of convergence, is expected

$$(1-\zeta)^b A(\zeta),$$
(42)

where $A(\zeta)$ is analytical in the current tip. The radius of convergence must not include other possible singularities. For a linear differential equation of order 2, a second linearly independent solution having the form

$$(1-\zeta)^d B(\zeta) \quad \text{or} \quad (1-\zeta)^b A(\zeta)\ln(1-\zeta) + C(\zeta)(1-\zeta)^d$$
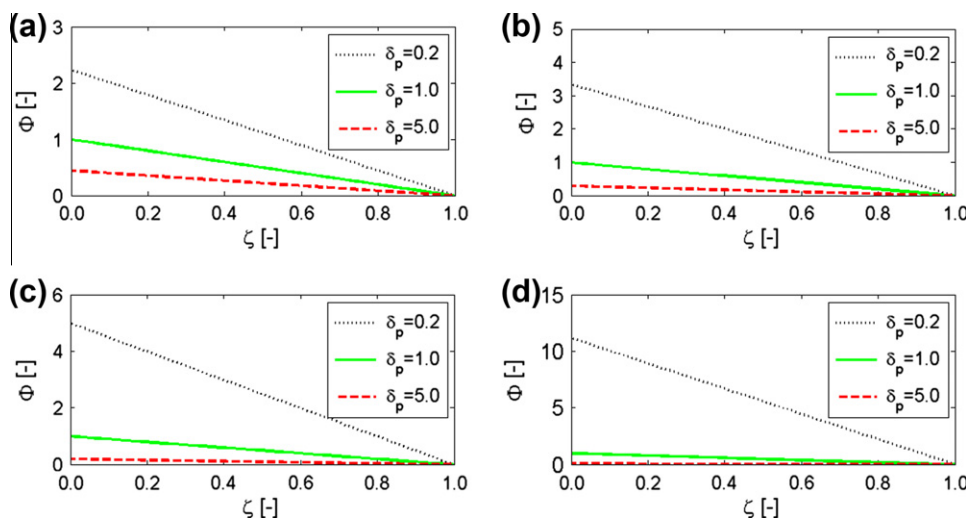(43)

Fig. 9. Shape factor for $\alpha = 2$ (Eq. (41)) for $\delta_p = 0.2, 1.0, 5.0$ and flow behavior index $n = 0.5$ (a), $n = 0.75$ (b), $n = 1$ (c) and $n = 1.5$ (d).

is expected, where $A(\zeta)$, $B(\zeta)$ and $C(\zeta)$ are analytic functions at $\zeta = 1$. While for a linear differential equation knowledge of two independent solutions implies the complete solution of the differential problem, this result is not guaranteed for a non-linear differential equation. Therefore, in addition to the analytical solutions (e.g. Eqs. (23) and (41)), there may still be other special solutions not obtained for any choice of the parameters.

In absence of known analytical solutions for generic α and n, two different approximations were presented. The first is a development in Frobenius series near the current tip and which holds also near the origin; the large range of validity of the approximation is due to the absence of other fixed or movable singularities, hence there are no limitations on the radius of convergence. The computation of the coefficients is cumbersome but can be handled to every order with symbolic software like Mathematica or Matlab.

The second is an iterative computation of a series in terms of α, which is an excellent approximation for small α but cannot be extended to too many iterations due to the difficulties in solving the integrals.

Our results demonstrate that the shape of the current is mostly sensitive to the rate of increase of injected volume and moderately to flow behavior index; for an instant release of fluid and for constant fluid inflow rate, the current length depends inversely on flow behavior index for early times ($T < 1$), and directly for late times ($T > 1$). The case of linearly increasing flow rate ($\alpha = 2$) acts as a transition between decelerating and accelerating currents.

References

[1] A.W. Woods, Liquid and vapor flow in superheated rock, Ann. Rev. Fl. Mech. 31 (1999) 171–199.
[2] S.E. King, A.W. Woods, Dipole solutions for viscous gravity currents: theory and experiments, J. Fluid Mech. 483 (2003) 91–109.
[3] D.M. Anderson, R.M. McLaughlin, C.T. Miller, The averaging of gravity currents in porous media, Phys. Fluids 15 (10) (2003) 2810–2829.
[4] M. Bickle, A. Chadwick, H.E. Huppert, M. Hallworth, S. Lyle, Modelling carbon dioxide accumulation at Sleipner: implications for underground carbon storage, Earth Planet. Sci. Lett. 255 (1–2) (2007) 164–176.
[5] M.A. Hesse, F.M. Orr, H.A. Tchelepi, Gravity currents with residual trapping, J. Fluid Mech. 611 (2008) 35–60.
[6] H.E. Huppert, A.W. Woods, Gravity-driven flows in porous layers, J. Fluid Mech. 292 (1995) 55–69.
[7] S. Lyle, H.E. Huppert, M. Hallworth, M. Bickle, A. Chadwick, Axisymmetric gravity currents in a porous medium, J. Fluid Mech. 543 (2005) 293–302.
[8] D. Vella, H.E. Huppert, Gravity currents in a porous medium at an inclined plane, J. Fluid Mech. 555 (2006) 353–362.
[9] D. Takagi, H.E. Huppert, Viscous gravity currents inside confining channels and fractures, Phys. Fluids 20 (2008) 023104.
[10] M. Golding, H.E. Huppert, The effect of confining impermeable boundaries on gravity currents in a porous medium, J. Fluid Mech. 649 (2010) 1–17.
[11] H.E. Huppert, The propagation of two-dimensional and axisymmetric viscous gravity currents over a rigid horizontal surface, J. Fluid Mech. 121 (1982) 43–58.
[12] H.E. Huppert, The intrusion of fluid mechanics into geology, J. Fluid Mech. 173 (1986) 557–594.
[13] J.E. Simpson, Gravity currents in the laboratory, atmosphere, and ocean, Ann. Rev. Fl. Mech. 14 (1982) 213–234.
[14] J.E. Simpson, Gravity Currents: In the Environment and the Laboratory, second ed., Cambridge University Press, 1997.
[15] M. Ungarish, An Introduction to Gravity Currents and Intrusions, CRC Press, 2010.
[16] Y.-S. Wu, K. Pruess, Flow of non-Newtonian fluids in porous media, Adv. Por. Med. 3 (1996) 87–184.
[17] R.P. Chhabra, J.F. Richardson, Non-Newtonian Flow in the Process Industries: Fundamentals and Engineering Applications, Butterworth, Heinemann, 1999.
[18] T. Sochi, Flow of non-Newtonian fluids in porous media, J. Polym. Sci.: Part B: Polym. Phys. 48 (2010) 2437–2767.
[19] S. Wang, Y. Huang, F. Civan, Experimental and theoretical investigation of the Zaoyuan field heavy oil flow through porous media, J. Pet. Sci. Eng. 50 (2006) 83–101.
[20] T. Babadagli, Development of mature oil fields – a review, J. Pet. Sci. Eng. 57 (3–4) (2007) 221–246.
[21] M.F. Nazar, S.S. Shah, M.A. Khosa, Microemulsions in enhanced oil recovery: a review, Pet. Sci.Technol. 29 (13) (2011) 1353–1365.
[22] D.A. Vallero, J. Peirce, Engineering the Risks of Hazardous Wastes, Butterworth, Heinemann, 2003.
[23] Y.L. Yan, Q. Deng, F. He, X.Q. Zhang, Y.-P. Liu, Remediation of DNAPL-contaminated aquifers using density modification method with colloidal liquid aphrons, Colloids Surfaces A: Physicochem. Eng. Aspects 385 (1–3) (2011) 219–228.
[24] T. Tosco, R. Sethi, Transport of non-Newtonian suspensions of highly concentrated micro- and nanoscale iron particles in porous media: a modeling approach, Environ. Sci. Technol. 44 (2010) 9062–9068.
[25] R.C. Bataller, On unsteady gravity flows of a power-law fluid through a porous medium, Appl. Math. Comput. 196 (2008) 356–362.
[26] J.P. Pascal, H. Pascal, Similarity solutions to gravity flows of non-Newtonian fluids through porous media, Int. J. Non-Linear Mech. 28 (2) (1993) 157–167.
[27] P.G. Saffman, G.I. Taylor, The penetration of a fluid into a porous medium or Hele-Shaw cell containing a more viscous liquid, Proc. Roy. Soc. London Set. A 245 (1958) 312–329.
[28] G.M. Homsy, Viscous fingering in porous media, Ann. Rev. Fluid Mech. 19 (1987) 271–311.
[29] A. Lindner, D. Bonn, E. Corvera Poiré, M. Ben Amar, J. Meunier, Viscous fingering in non-Newtonian fluids, J. Fluid Mech. 469 (2002) 237–256.
[30] S. Mora, M. Manna, Saffman–Taylor instability for generalized Newtonian fluids, Phys. Rev. E 80 (2010) 016308.
[31] R.B. Bird, W.E. Stewart, E.N. Lightfoot, Transport Phenomena, Wiley, 1960.
[32] R.H. Cristopher, S. Middleman, Power-law flow through a packed tube, Ind. Eng. Chem. Fundam. 4 (4) (1965) 422–427.
[33] J.G. Savins, Non-Newtonian flow through porous media, Ind. Eng. Chem. Fundam. 6 (10) (1969) 18–47.
[34] D. Teeuw, F.T. Hesselink, Power-law flow and hydrodynamic behavior of biopolymer solutions in porous media, Soc. Pet. Eng. Paper Number SPE 8982, Fifth International Symposium on Oilfield and Geothermal Chemistry, Stanford, California, 1980, pp. 73–86.
[35] H. Pascal, Nonsteady flow of non-Newtonian fluids through porous media, Int. J. Eng. Sci. 21 (3) (1983) 199–210.
[36] K. Velten, A. Lutz, K. Friedrich, Quantitative characterization of porous materials in polymer processing, Compos. Sci. Technol. 59 (1999) 495–504.
[37] G.B. Kim, J.M. Hyun, Buoyant convection of a power-law fluid in an enclosure filled with heat-generating porous media, Numer. Heat Transfer, Part A: Appl. 45 (6) (2004) 569–582.
[38] K. Vajravelu, S. Sreenadh, G. Viswanatha Reddy, Helical flow of a power-law fluid in a thin annulus with permeable walls, Int. J. Non-Linear Mech. 41 (2006) 761–765.
[39] G. Degan, K. Akowanou, N.C. Awanou, Transient natural convection of non-Newtonian fluids about a vertical surface embedded in an anisotropic porous medium, Int. J. Heat Mass Transfer 50 (2007) 4629–4639.
[40] R.G. Larsson, Derivation of generalized Darcy equations for creeping flow in porous media, Ind. Eng. Chem. Fundam. 20 (1981) 132–138.
[41] A.V. Shenoy, Non-Newtonian fluid heat transfer in porous media, Adv. Heat Transfer 24 (1995) 102–190.
[42] D.A. Nield, A. Bejan, Convection in Porous Media, third ed., Springer, 2006.
[43] T.S. Lundstrom, H. Sundlof, J.A. Holmberg, Modeling of power-law fluid flow through fiber beds, J. Compos. Mater. 40 (3) (2006) 283–296.
[44] I.M.R. Sadiq, R. Usha, Effect of permeability on the instability of a non-Newtonian film down a porous inclined plane, J. Non-Newton. Fluid Mech. 165 (2010) 1171–1188.
[45] A. Barletta, D.A. Nield, Linear instability of the horizontal throughflow in a plane porous layer saturated by a power-law fluid, Phys. Fluids 23 (2011) 013102.
[46] M. Vakilha, M.T. Manzari, Modelling of power-law fluid flow through porous media using smoothed particle hydrodynamics, Transp. Por. Med. 74 (2008) 331–346.
[47] M.T. Balhoff, K.E. Thompson, A macroscopic model for shear-thinning flow in packed beds based on network modeling, Chem. Eng. Sci. 61 (2006) 698–719.
[48] A. Fadili, P.M.J. Tardy, A. Pearson, A 3D filtration law for power-law fluids in heterogeneous porous media, J. Non-Newton. Fluid Mech. 106 (2002) 121–146.
[49] V. Di Federico, M. Pinelli, R. Ugarelli, Estimates of effective permeability for non-Newtonian fluid flow in randomly heterogeneous porous media, Stoch. Environ. Res. Risk Assess. 24 (2010) 55–69.
[50] V. Di Federico, S. Cintoli, S. Malavasi, Viscous spreading of non-Newtonian gravity currents on a plane, Meccanica 41 (2) (2006) 207–217.
[51] L. Li, D.A. Lockington, M.B. Parlange, F. Stagnitti, D.S. Jeng, J.S. Selker, A.S. Telyakovskiy, D.A. Barry, J.Y. Parlange, Similarity solution of axisymmetric flow in porous media, Adv. Water Resour. 28 (10) (2005) 1076–1082.
[52] C.M. Bender, S.A. Orszag, Advanced Mathematical Methods for Scientists and Engineers, McGraw-Hill, 2008.

ERRATA-CORRIGE

Equation 3 p.47 is erratum:

$$\frac{k}{\mu_{ef}} = \frac{1}{2m}\left(\frac{n\phi}{3+n}\right)^{n}\left(\frac{8k}{\phi}\right)^{(1+n)/2} , \tag{3}$$

The rectification is:

$$\frac{k}{\mu_{ef}} = \frac{1}{2m}\left(\frac{n\phi}{3n+1}\right)^{n}\left(\frac{8k}{\phi}\right)^{(1+n)/2} , \tag{3}$$